Nanoscale Advances

ROYAL SOCIETY OF CHEMISTRY

MINIREVIEW

View Article Online
View Journal | View Issue

Cite this: *Nanoscale Adv.*, 2023, **5**, 615

Advances in high-voltage supercapacitors for energy storage systems: materials and electrolyte tailoring to implementation

Jae Muk Lim,†[a] Young Seok Jang,†[a] Hoai Van T. Nguyen,†[b] Jun Sub Kim,†[a] Yeoheung Yoon,[c] Byung Jun Park,[c] Dong Han Seo, *[a] Kyung-Koo Lee, *[b] Zhaojun Han, *[d] Kostya (Ken) Ostrikov [ef] and Seok Gwang Doo*[a]

To achieve a zero-carbon-emission society, it is essential to increase the use of clean and renewable energy. Yet, renewable energy resources present constraints in terms of geographical locations and limited time intervals for energy generation. Therefore, there is a surging demand for developing high-performance energy storage systems (ESSs) to effectively store the energy during the peak time and use the energy during the trough period. To this end, supercapacitors hold great promise as short-term ESSs for rapid power recovery or frequency regulation to improve the quality and reliability of power supply. In particular, the electrical double layer capacitor (EDLC) which offers long and stable cycle retention, high power densities, and fast charge/discharge characteristics with a moderate operating voltage window, is a suitable candidate. Yet, for implementation of the EDLC in ESSs, further research effort is required in terms of increasing the operating voltage and energy densities while maintaining the long-term cycle stability and power densities which are desirable aspects for ESS operation. Here, we examine the advances in EDLC research to achieve a high operating voltage window along with high energy densities, covering from materials and electrolytes to long-term device perspectives for next-generation supercapacitor-based ESSs.

Received 28th November 2022
Accepted 20th December 2022

DOI: 10.1039/d2na00863g

rsc.li/nanoscale-advances

1. Introduction

Recently, the concept of an RE100 society has become an important initiative around the globe, due to the significant effect of global warming and climate change, and it aims to supply 100% of the electricity required for the industry with renewable energy (RE).[1] However, diverse sources of renewable energy such as wind, hydropower, solar and geothermal, are often intermittent in nature and pose spatial and geographical constraints for implementation. Therefore, the use of various forms of energy storage systems (ESSs) capable of storing the oversupplied or residual energy generated by renewable energy sources during peak times has become a topic of significant importance. For ESSs, various energy storage devices are used including rechargeable batteries, redox flow batteries, fuel cells and supercapacitors.[2–4] Typically, for a short- to mid-term electrical power supply, batteries and capacitors are considered as favorable energy storage devices whereas supercapacitors (SCs, also known as electrochemical capacitors) are considered for the power stabilization and frequency regulatory purposes to improve the power quality and batteries that are being considered to supply stable electrical power for a longer duration.[5] A supercapacitor is a favorable energy storage device for rapid power recovery purposes due to advantageous features such as fast charge/discharge characteristics, superior power density, semi-permanent cycle life, low holding cost, fast response characteristics, and high stability. Yet, commercial electrical double layer capacitor (EDLC) based supercapacitors exhibit low energy densities and a moderate operating voltage window, which leads to large numbers of cells being connected in series to achieve the desired power and meet the energy demand, ultimately increasing the production cost of the supercapacitor-based ESS.[6] Therefore, continuous research efforts are needed in terms of increasing energy densities and widening the operating voltage window of the EDLC devices.[7] Supercapacitors can be classified into three types: (1) EDLCs, (2) pseudocapacitors, and (3) hybrid

[a]*Energy Materials & Devices, Department of Energy Engineering, Korea Institute of Energy Technology (KENTECH), Naju-si (58217), Jeollanam-do, Republic of Korea. E-mail: dhseo@kentech.ac.kr; sgdoo@kentech.ac.kr*

[b]*Department of Chemistry, Kunsan National University, Gunsan-si (54150), Jeollabuk-do, Republic of Korea. E-mail: kklee@kunsan.ac.kr*

[c]*New & Renewable Energy Laboratory, Korea Electric Power Corporation (KEPCO) Research Institute, 105 Munji-ro, Yuseong-gu, Daejeon 34056, Republic of Korea*

[d]*School of Chemical Engineering, The University of New South Wales, Kensington, New South Wales 2052, Australia. E-mail: Zhaojun.han@unsw.edu.au*

[e]*School of Chemistry and Physics and QUT Centre for Materials Science, Queensland University of Technology (QUT), Brisbane, Queensland 4000, Australia*

[f]*ARC Centre of Excellence for Carbon Science and Innovation, Queensland University of Technology (QUT), Brisbane, Queensland 4000, Australia*

† These authors contributed equally to this work.

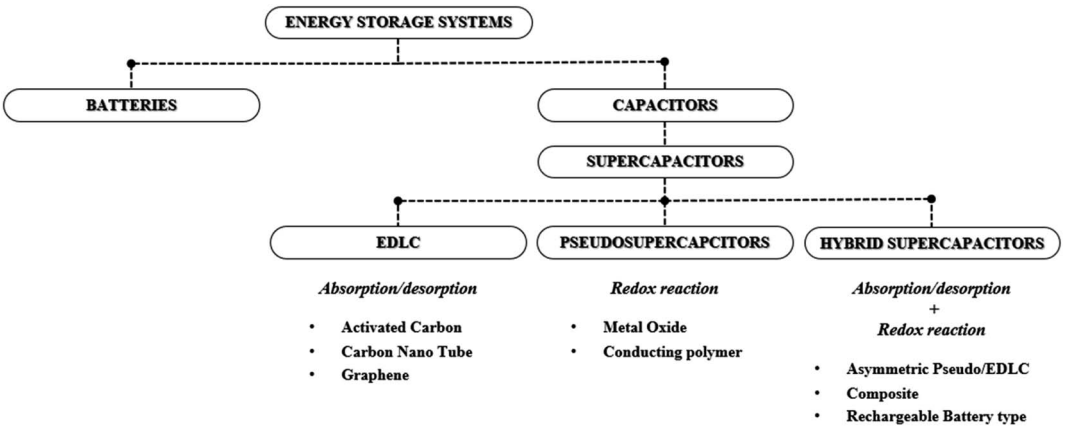

Fig. 1 Summary of supercapacitor types and electrode material systems.

supercapacitors.[8] (Fig. 1) Amongst the three types of capacitors, EDLC-based supercapacitors are considered the most appropriate for the ESSs as the EDLC offers the most stable charge storage capability for long-term cycling which is the most important criterion for fabricating high performance and stable ESSs. Therefore, this minireview aims to review and discuss advances in EDL-based supercapacitors for their practical implementation in ESSs with the perspectives of critical parameters which determine the operating voltage window, energy and power densities, along with long-term cycle stability.

2. Fundamentals of supercapacitors

A supercapacitor is a type of capacitor having a large charge storage capacity and is also known as an ultra-capacitor. Unlike batteries which rely on electrochemical reactions, supercapacitors utilize surface charge adsorption or surface/partial redox reactions as charge storage mechanisms and more recently a hybrid mechanism involving both an electrochemical reaction and surface charge adsorption. Moreover, depending on the charge storage mechanism, various types of materials are used in different types of supercapacitors.[9] As for this minireview's focus, the concept of an electrical double layer capacitor was first introduced by Helmholtz in the 1800s. The working principle of the EDLC is based on electrostatic charge adsorption. Carbon-based active materials such as activated carbon (AC), carbon nanotubes (CNTs) and graphenes are typically exploited as symmetrical electrodes for EDLCs.[10] In an EDLC, by forming an electrical double layer, electrochemical energy is stored in the layer which is formed at the interface between the electrodes and electrolytes. With non-faradaic reaction mechanisms, ions in electrolytes are electrostatically adsorbed on the surfaces of electrodes during charging. Induced charges are accumulated in the electrical double layer formed at the interface between the electrode and the electrolyte. The ions adsorbed on the surface or the pores of the active materials diffuse back into the electrolyte while discharging. Since no chemical reaction occurs during the charge/discharge, for this reason, EDLCs exhibit high power density and excellent cycle stability, and have stable operation even in a low-temperature environment.

Unlike EDLCs, pseudocapacitors rely on the electrochemical surface redox reaction mechanism and often utilize metal oxide-based materials or conductive polymers as the electrode material in a symmetrical configuration.[10] In pseudocapacitors, ions in the electrolyte induce charge transfer on the surface of the active materials during the charging and discharging processes without involving the state change of the active materials. Though pseudocapacitors promise higher specific capacitance and energy densities, due to involvement of the surface redox reaction, they exhibit lower cycling stability and power densities compared to EDLCs which are disadvantageous when implementing them in ESSs. Hybrid supercapacitors utilize asymmetric electrodes consisting of both metal oxide (for an intercalative or redox reaction) and carbon material electrodes (for surface ion adsorption); where one electrode exhibits high-capacity characteristics, while the other exhibits high-power characteristics thus aiming to obtain both high energy and power densities.[10] Similar to the pseudocapacitors, hybrid capacitors promise high energy densities with a high operating voltage window, yet, due to the presence of a battery-like electrode, they exhibit poor cycling stability and low power densities and are not yet suitable for implementation in ESSs and further research effort is needed to improve their cycling stability and power densities.[11] (Fig. 2) Therefore, currently, EDLCs show great potential for implementation in ESSs given that the energy densities and the operating voltage window can be improved.

In the EDLC, there are a few important parameters affecting the total energy stored in the device including the capacitance of the active materials and the operating voltage window, which can be represented by the following equations:

$$C = \frac{Q}{V} = \frac{\varepsilon_r * \varepsilon_0 * A}{d} \quad E = \frac{1}{2} C V^2$$

where C is the capacitance, Q is the total charge, V is the voltage, ε_r is the relative permittivity, ε_0 is the permittivity of free space, A is the surface area of the electrode, and d is the distance between two opposite electrodes. E represents the energy, V is the voltage and C is the capacitance of the device. According to the above equations, to improve the energy densities, one can either increase the specific capacitance which is strongly related

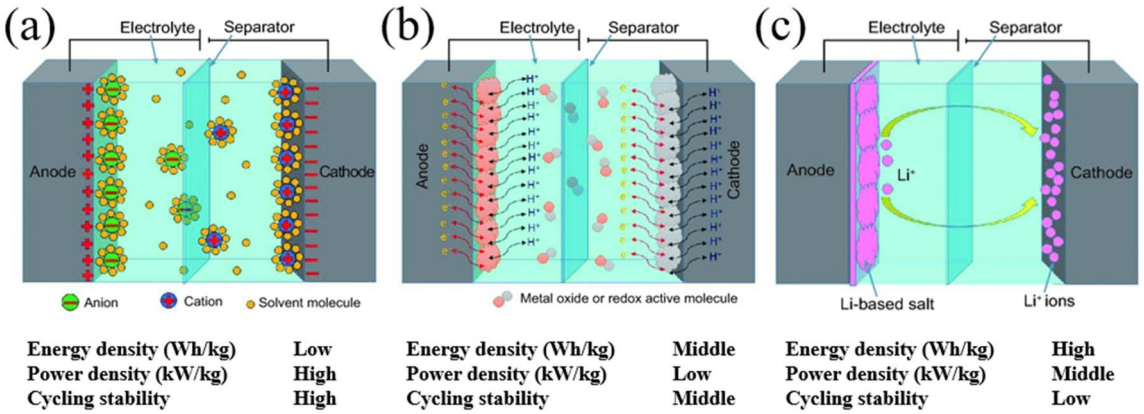

Fig. 2 Schematic of (a) an electrical double-layer capacitor (EDLC), (b) a pseudocapacitor, and (c) a hybrid supercapacitor.[10] [This figure has been adapted/reproduced from ref. 10 with permission from OXFORD UNIVERSITY PRESS, copyright 2017.]

Table 1 Various types of electrolytes used in supercapacitors and their characteristics.[13] [This figure has been adapted/reproduced from ref. 13 with permission from Elsevier, copyright 2021.]

	Aqueous	Organic	Ionic liquid
Stable potential window (V)	0.8–2.0	2.5–2.8	3.5–4.5
Ionic conductivity	High	Middle	Low
Cost	Low	Middle	High
Manipulability	Simple	Complex	Middle
Flammability	None	High	Middle
Toxicity	None	High	Low
Volatility	Middle	High	Low
Chemical/thermal stability	Middle	Low	High

to the material's intrinsic properties such as the material's surface area or one can increase the operating voltage window which is strongly related to the characteristics of the electrolyte. The stronger influence on the energy density is imposed by the characteristics of the electrolytes. Electrolytes can be divided into three categories including: (1) aqueous, (2) organic, and (3) ionic liquid (IL) electrolytes (Table 1).[12] Aqueous electrolytes exhibit a limited voltage window where water breaks down at the potential window beyond 1.23 V whereas, IL electrolytes offer the highest operating voltage window yet their low ionic conductivity leads to lower power densities as well as requiring elevation of temperature for their effective operation. Moreover, the high cost of IL electrolytes poses a challenge for their commercialization.

Therefore, organic electrolyte-based EDLC supercapacitors which offer a moderate operating voltage window, are the most widely commercialized form with the highest chance of being implemented in ESSs, which will be a major focus of this minireview.

3. Electrolyte perspectives for high-voltage EDLC-type supercapacitors

Electrolytes have critical importance in improving the energy densities and widening of operating voltages and the long-term stability of SCs, as their physicochemical and electrochemical properties significantly affect the overall performance of SCs.

The relative comparison of several important aspects of the three categories of electrolytes is plotted in Fig. 3.[14,15] It is well known that the cell voltage is mainly limited by the electrochemical stability window (ESW) of electrolytes. The ESW of electrolytes, defined as the gap between the reduction and oxidation potentials, is influenced by the nature of ions (cations and anions), solvent molecules, and the interaction between ion–ion, ion–solvent and the electrode surface–electrolyte.[16] To achieve high-voltage EDLC-based SCs, electrolytes based on ILs and organic solvents are more widely used than the aqueous electrolytes because of their wider ESW. However, different ESWs of the same electrolyte can be observed since it is significantly related to the electrode materials employed.[17] Usually, the ESW of an electrolyte achieved on inert electrodes (*i.e.*, platinum and glassy carbon) is broader than that on porous carbon electrodes, due to the presence of abundant functional groups on the carbon surface.[14,18] Therefore, the purity level of electrode materials and the presence of functional groups on the active materials, and the physicochemical stability of the

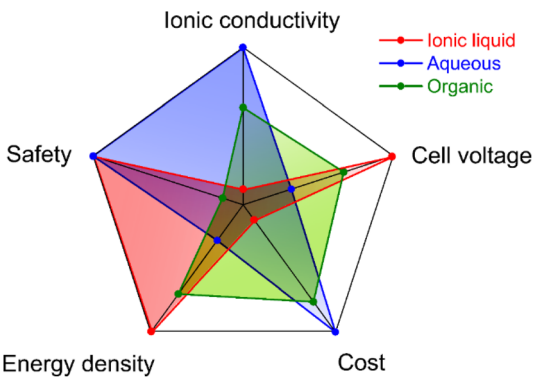

Fig. 3 Comparison of the properties and performance of IL, aqueous, and organic electrolytes. Reproduced from ref. 14 [this figure has been adapted/reproduced from ref. 14 with permission from the Royal Society of Chemistry, copyright 2021].

active materials do play an important role in determining the ESW of an electrolyte.[16] Hence, rational design of electrolytes, active materials and the electrode material is critical for developing high-voltage EDLCs.

3.1 Aging mechanisms of common electrolytes in SCs at a high operating voltage

Long-term stability is one of the most important parameters to be considered for high performance ESSs. Under the high-voltage or high-temperature operation of SCs, irreversible electrochemical processes can occur in the devices, resulting in capacitance loss and an increase in the equivalent series resistance, which negatively impact the long-term stability of the SCs. Many articles proposed that the decomposition of electrolyte by the impurities or functional groups on the carbon-based active material can strongly affect the aging of electrolytes for SCs, especially at a high operating voltage.[19–21] The electrolyte decomposition products may block the pores, which leads to a significant decrease in the specific surface area and pore volume of the SCs.[22,23] In previous studies, it was demonstrated that the ions in widely used electrolytes such as the alkylammonium cation could decompose at a high working voltage into ethylene, trialkylamine, and hydrogen fluoride through reaction 1.[20,24]

$$[(CH_3CH_2)_4N]^+ + F^- \rightarrow (CH_3CH_2)_3N + H_2C{=}CH_2 + HF \quad (1)$$

On the other hand, other widely used ions such as BF_4^- can hydrolyze in the presence of trace amounts of water in the SCs, which decompose into hydrogen fluoride, fluoride, and boric acid derivatives (reactions 2–5):[20]

$$BF_4^- \rightarrow BF_3 + F^- \quad (2)$$

$$BF_3 + HF \rightarrow HBF_4 \quad (3)$$

$$HBF_4 + H_2O \rightarrow HBF_3(OH) + HF \quad (4)$$

$$4BF_3 + 3H_2O \rightarrow B(OH)_3 + 3HBF_4 \quad (5)$$

The widely used solvent for electrolytes such as acetonitrile (AN) can also decompose under high-voltage conditions to various products through hydrolysis reaction (6), hydrohalogenation (7), or polymerization reactions (8) and (9).[20,21,24]

$$CH_3C{\equiv}N \xrightarrow{H_2O} CH_3CONH_2 \xrightarrow{H_2O} [CH_3COO]NH_4 \quad (6)$$

$$CH_3C{\equiv}N \xrightarrow{HF} FCH_3C{=}NH \xrightarrow{HF} CH_3CF_2NH_2 \quad (7)$$

$$CH_3C{\equiv}N \xrightarrow{BF_4^-} \dot{C}H_2\,C{\equiv}N + H^+ + BF_4^- \quad (8)$$

$$\dot{C}H_2C{\equiv}N + nCH_3C{\equiv}N \rightarrow H(N{=}C(CH_3))_n{-}HN{=}CH(CH_3) \quad (9)$$

Similarly, for other widely used solvents such as propylene carbonate (PC), the electrochemical oxidation and reduction could occur under high-voltage conditions (3.7–4.0 V) to generate CO_2 gas, propene, and poly-PC, while at the lower cell voltage (3.0–3.7 V), the CO_2 and CO gas, and adsorbed water can be released through the gasification of oxygen-containing functional groups on the active material surface on the positive electrode. On the other hand, H_2, CO, CO_2, ethylene, trialkylamine, and propylene glycol, can be generated on the negative electrode.[21,25] Therefore, controlling the impurities and functional groups on the electrode material and the ESW of the electrolyte is crucial for enhancing the long-term stability, operating voltage window and energy densities.

3.2 The use of electrolytes with high electrochemical stability

In regard to improving the ESW of the organic electrolytes, intense research efforts have been made to explore alternative solvents with a wider ESW compared to the conventional AN-, and PC-based solvents, such as adiponitrile (ADN),[26] 2,3-butylene carbonate (2,3-BC),[27] ethyl isopropyl sulfone (EiPS),[28] and propionitrile (PN).[29] For example, the ESW of 0.7 M $TEABF_4$/ADN is as high as 3.75 V, where ADN-based electrolyte could operate without any detrimental effect at a cell voltage of 3.5 V over 35 000 cycles. Chiba *et al.*[27,28] demonstrated the use of 2,3-BC and EiPS electrolytes to endow SCs with a high operating voltage up to 3.5 V. This was attributed to the high stability of these electrolytes at the AC electrode/electrolyte interface at a high operating potential. However, these electrolytes usually possess low ionic conductivity and high viscosity, resulting in limited power density. Interestingly, a recent study suggests that the PN-based electrolyte also allows the SCs to operate at a cell voltage of 3.5 V with excellent ionic conductivity and low viscosity (1 M 1,1-dimethylpyrrolidinium tetrafluoroborate ($DMPBF_4$)/PN: 25.3 mS cm^{-1}, 1.01 cP).[29] This is due to the higher oxidation potential with a more symmetric electrochemical stability window of PN-based electrolytes compared to AN-based electrolytes. The PN-based electrolyte exhibits great attributes for outstanding performances in terms of the viscosity, ionic conductivity, cell working voltage, and cycling performance. To increase the SC operating voltage, ILs as solvent-free electrolytes have been receiving much attention from researchers. Electrolytes such as *N*-butyl, *N*-methyl-pyrrolidinium bis(trifluoromethanesulfonyl)imide ($Pyr_{14}TFSI$), *N*-methyl, *N*-butyl-azepanium bis(trifluoromethanesulfonyl) imide ($Azp_{14}TFSI$), and *N*-methyl, *N*-hexyl-azepanium bis(trifluoromethanesulfonyl)imide ($Azp_{16}TFSI$) were reported to exhibit a similar operating potential window, resulting in stable SC operation up to 3.5 V at 60 °C without significant capacitance fading after 35 000 cycles.[30] However, these ILs have the main disadvantages of high viscosity, low ionic conductivity, and high cost. Martins *et al.*[31] found that the use of ILs containing tetracyanoborate anions ($[B(CN)_4]^-$) could provide a maximum operating voltage of 3.7 V while maintaining high ionic conductivity at 25 °C ($Pyr_{14}B(CN)_4$: 6.9 mS cm^{-1}). Therefore, the SCs using $Pyr_{14}B(CN)_4$ electrolyte exhibited high specific capacitances of 20 F g^{-1} even at a high rate of 15 Ag^{-1} and could retain >75% capacitance retention after 50 000 cycles (at a current density of 2.0 A g^{-1}) at 3.7 V.

3.3 Design strategies for high-voltage electrolytes for SCs

To attain a higher working voltage for the EDLC, inhibiting the electrolyte decomposition reactions on porous carbon active materials at high potential is essential. Apart from the above-mentioned approaches, other methods have been attempted to develop suitable electrolytes for high-voltage SCs including the incorporation of electrolyte additives to form a passivation layer for preventing further electrolyte decomposition, and modulating electrolyte components to adjust the potential to zero voltage (E_{0V}).

3.3.1 Formation of a passivation layer on the electrode. In lithium-ion batteries, the stability of the cells relies on the formation of a passivation layer called the solid electrolyte interphase (SEI), which acts as the protective layer to prevent irreversible redox reactions between the electrolyte and electrode. A similar concept can be considered for SCs. The operating voltage was expected to extend by forming a passivation layer on the carbon electrode. Pohl *et al.*[32] found that after careful electrode surface passivation by gradually widening the potential range from 3.0 V to 3.7 V, the EDLCs based on titanium carbide-derived carbon electrodes and 1 M triethylmethylammonium tetrafluoroborate $(C_2H_5)_3CH_3NBF_4$/AN electrolyte were stabilized. The passivation effect can be explained by the redox reaction of the amorphous region in active carbon sites forming a thin passivation layer. Nguyen *et al.*[33] demonstrated that the working voltage of EDLCs based on bis(oxalate)borate (BOB)-containing electrolytes could even reach 4.0 V for 2000 cycles at a high temperature of 45 °C. This is attributed to the formation of a passivation layer comprising trigonal borates (B_2O_3 or H_3BO_3) and a semicarbonate species (O–C=O) on the negative electrode, preventing further electrolyte decomposition during the cycling.

Another effective way to form the effective passivation layer is to use fluorinated co-solvents and electrolyte additives. However, designing or choosing appropriate co-solvents and additives still remains a challenge. Krause *et al.*[34] have screened various additives and co-solvents for their ability to enhance cycling performance at higher voltages. Among the candidates, the addition of lithium difluoro(oxalato)borate (LiDFOB) or the tris(2,2,2-trifluoroethyl) phosphite (TTFEPi) additive into spiro-(1,1′)-bipyrrolidinium tetrafluoroborate ($SBPBF_4$)/AN improves the cycling performance during floating at a voltage of 3.5 V. It was explained by the presence of the additive which minimized the AN polymerization. Furthermore, by adding a fluorinated ether 1,1,2,2-tetrafluoroethyl-2,2,3,3-tetrafluoropropylether (TTE) in $(C_2H_5)_3CH_3NBF_4$/AN solution, Yao *et al.*[35] observed improved cycling stability at an operating voltage of 3.6 V, which was much higher than that of the operating voltage (2.7–3.0 V) of AN-based electrolyte without additives.

3.3.2 Modulation of electrolyte components to adjust the potential of zero voltage (E_{0V}). When a symmetric SC is assembled, the device's maximum voltage is always lower than the expected voltage stability window of the electrolytes. One of the main reasons for this is that the operating potential range of the negative and positive electrodes is not the same. In other words, the E_{0V} of the electrodes is not in the middle of the electrolyte stability window. In this case, the stability limit of the SC is reached as soon as one of the electrodes reaches the potential where faradaic processes start to occur. Therefore, the positive or negative electrode may not fully utilize the ESW of the given electrolyte system. One of the effective methods is modulating the electrolyte composition. Gogotsi *et al.*[36] reported that SCs based on onion-like carbon (OLC) electrodes and mixed electrolyte of 1-ethyl-3-methylimidazolium bis(trifluoromethylsulfonyl)imide (EMITFSI) and 1-ethyl-3-methylimidazolium tetrafluoroborate ($EMIMBF_4$) with the volume ratio of 4 : 1 could exhibit more symmetric potential ranges for positive and negative electrodes in comparison to the single IL electrolyte. This suggests that the symmetric potential range of electrodes can be adjusted by adding an appropriate amount of the new anion into the base electrolyte where similar strategies can be applied for the organic electrolyte case.

As discussed above, high ESW, high ionic conductivity and low viscosity of the electrolyte are the important factors affecting the SC performance under high-voltage conditions. Moreover, developing new additives which can enhance the ESW along with finding a cost-effective and organic electrolyte with less toxicity would be an important direction for future research.

4. Materials for high-voltage EDLC-based supercapacitors

4.1 Activated carbon

Activated carbon (AC) is one of the most widely used active materials in the supercapacitor industry owing to its large surface area, high porosity which determines the amount of charges that can be stored in the active materials and low-cost which are advantageous attributes for EDLCs.[37] AC can be obtained by thermal-based carbonization and activation processes of biomass-based materials such as coconut shell, starch, and wheat straw and petroleum-based pitch, coke or coal.[38] It is well known that AC can exhibit high specific surface areas of 2000 $m^2\ g^{-1}$ with abundant micropores (<2 nm) and mesopores (2–50 nm) which facilitates ion adsorption into these various pore structures.[39] For instance, Kierzek *et al.* reported the synthesis of AC with a specific surface area of 3150 $m^2\ g^{-1}$ using coal as a precursor,[40] and Balathanigaimani *et al.* reported corn grain-derived AC with a specific surface area of 3200 $m^2\ g^{-1}$.[41] The capacitance and diffusivity of charge carriers into active materials are strongly influenced by the specific surface area of active materials and pore structures (Fig. 4).[42] In particular, for the high-voltage SCs, utilizing organic electrolytes (organic solvents and ions) with large ionic radius would preferably require an active material with abundance of mesopores and high porosity to facilitate the charge storage.[43] However, as the pore size and density increase, the active material density could decrease which in turn results in a lower energy density of SCs. More importantly, AC with a high degree of sp^3 configuration reduces the electrical conductivity. Furthermore, AC often contains a large degree of functional groups which could lead to detrimental effects when operating under high-voltage conditions,

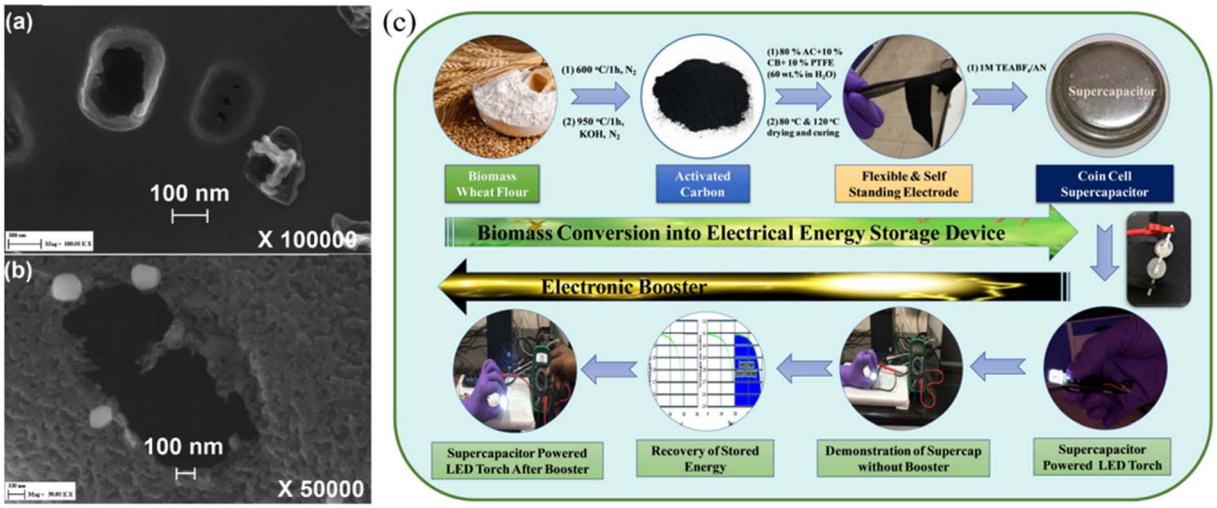

Fig. 4 (a) and (b) SEM images of activated carbon by CO_2 activation at 800 °C and by H_2O activation at 700 °C[42] and (c) schematic representation of conversion of wheat flour into a high energy density supercapacitor electrode with an additional booster circuit for the recovery of stored energy as a proof of concept.[44] [This figure has been adapted/reproduced from ref. 42 and ref. 44 with permission from Elsevier, copyright 2018 and from John Wiley and Sons, copyright 2020.]

as functional groups can induce undesirable decomposition of electrolyte. Therefore, control of the surface area, pore size distribution, conductivity and the degree of functional groups present in AC is crucial for achieving high-voltage SCs for ESSs.

To achieve high-performance SCs at high operating voltages using AC, various strategies were implemented including the heteroatom doping, varying raw precursor materials and activation methods.[45] Gandla *et al.* reported the synthesis of highly mesoporous, N-doped dragon fruit peel-derived AC with the addition of a melamine precursor as a source of nitrogen dopant, where KOH was used as an activation agent. The N-doped dragon fruit peel-derived AC exhibited a specific capacitance of 53 F g^{-1} with 109% capacitance retention after 5000 charge–discharge cycles at a high operating voltage of 3.5 V using 1 M $TEABF_4$/acetonitrile as the electrolyte (Fig. 5). Recently, Vijayakumar *et al.* reported an AC synthesis process stemming from bio-renewable precursors such as, wheat flour. Wheat flour-derived AC showed a high specific surface area of 1620 m^2 g^{-1} with a high mesopore content and the device made using AC demonstrated stable operation up to 3.2 V, with excellent cycling stability of 95% capacitance retention after 15 000 cycles and a high volumetric capacitance of 86 Fcm^{-3} (Fig. 4).[44] Guo *et al.* explored the impact of varying activation processes on the pore size distribution of AC using different activation agents such as NaOH and KOH using rice husk as a raw material. The result showed that NaOH-based activation agents were more effective in generating a higher degree of mesopores compared to the conventional KOH-based activation agents which would be useful for implementation in high-voltage SCs. Moreover, NaOH activation agents lead to increased specific surface area (2721 m^2 g^{-1}) compared to the KOH agent (1930 m^2 g^{-1}).[46] Therefore, to utilize AC in high-voltage SCs, one needs to carefully optimize the synthesis of AC from the selection of raw precursor materials to controlling the carbonization and the pore-generating activation process to achieve AC with higher mesoporosity compared to AC with microporosity with minimum degree of amorphous carbon and functional groups, which are all critical material parameters for long-term stability of AC-based SCs under high-voltage conditions.

4.2 Carbon nanotubes

One-dimensional carbon-based nanomaterials such as carbon nanotubes (CNTs), are another widely used candidate for active materials for EDLCs. CNTs consist of carbon atoms arranged in a hexagonal lattice which are rolled up to form a tubular shape. Due to the high sp^2 carbon content, CNTs exhibit very high electrical conductivity.[47] Moreover, CNTs do not contain a high degree of functional groups, as they are often synthesized *via* non wet-chemistry-based techniques such as arc discharge, pulsed laser vaporization, and chemical vapor deposition (CVD) using purified gaseous precursors. Moreover, CNTs can be directly synthesized on the current collector which makes easy integration without the need of binders.[11] CNTs can also be divided according to the number of enclosed walls, such as single-wall carbon nanotubes (SWCNTs) and multi-wall carbon nanotubes (MWCNTs) and exhibit varying electrical properties according to the diameter and symmetry of the nanotubes.[48] Moreover, CNTs exhibit a moderate specific surface area (~600 m^2 g^{-1}) with great mechanical and physicochemical stability which is advantageous for high-voltage SCs.[49,50] In addition, SWCNTs or few-walled CNTs with a higher specific surface area with enhanced conductivity compared to the MWCNTs, are the preferred form for energy storage devices. In CNT-based SCs, under high-voltage conditions, SC performance can be strongly influenced by the degree of impurities.[51] In particular, the metallic impurities arising from the necessity of a metal catalyst for CNT growth and the amorphous carbons that could form

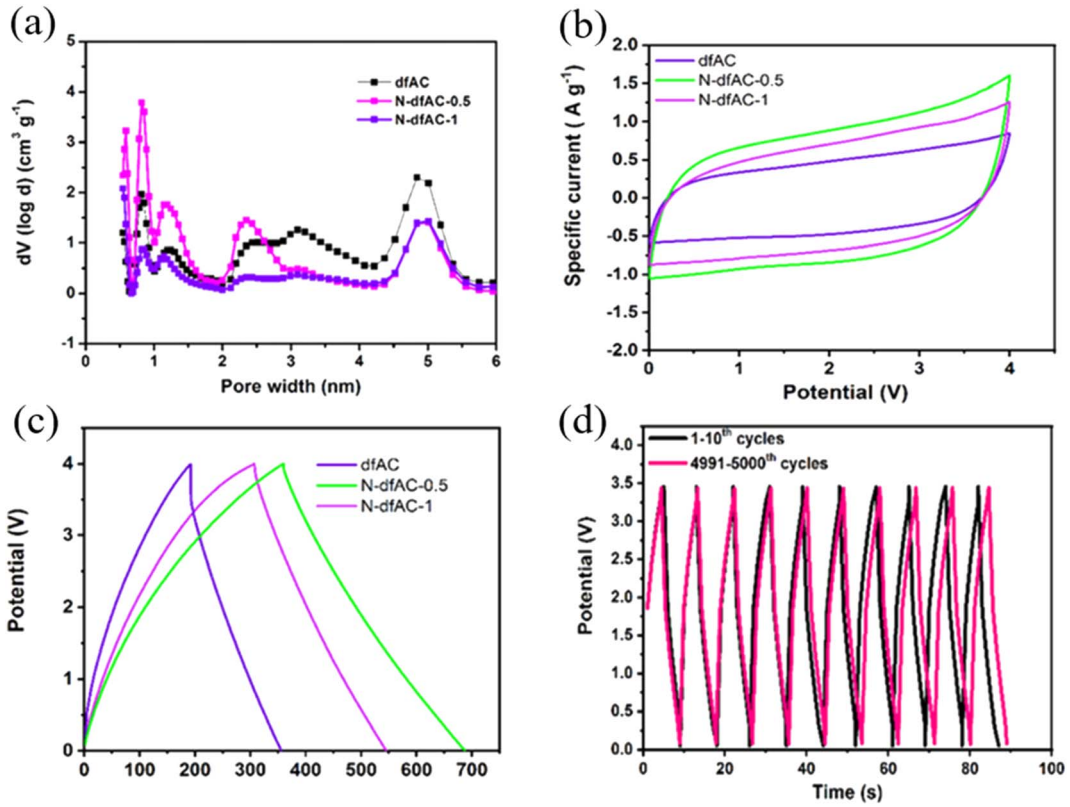

Fig. 5 (a) Pore size distribution of micropores to mesopores and (b) CV curves of the N-doped mesoporous-dominated hierarchical activated carbon electrode at a scan rate of 25 mV s^{-1}, respectively. (c) Galvanostatic charge/discharge curves of the N-doped mesoporous activated carbon derived from dragon fruit peel at a constant current density of 3 mA cm^{-2} and (d) long-term cycling performance up to 5000 cycles at a constant current density of 50 mA cm^{-2}.[45] [This figure has been adapted/reproduced from ref. 45 with permission from American Chemical Society, copyright 2021.]

during the growth are common in CNT synthesis which could undergo unwanted side reactions with electrolyte, degrading the long-term stability of SCs (Fig. 6).[51] To avoid such impurity issues, Izadi *et al.* by carefully controlling the iron catalyst size distribution on the Si substrate along with the well-controlled water-assisted CVD process, demonstrated the synthesis of a vertically aligned CNT forest with SWCNT-dominant, low amorphous carbon contents. During the CNT forest removal, metallic impurities were bound to the substrate and did not attach on the CNTs. After the liquid-induced densification process of SWCNTs, a mesoporous CNT-based active material electrode was prepared, which showed stable SC operation at 4 V with a high capacitance retention (96.4%) over 1000 cycles at a current density of 1 A g^{-1} from 0 V to 4 V.

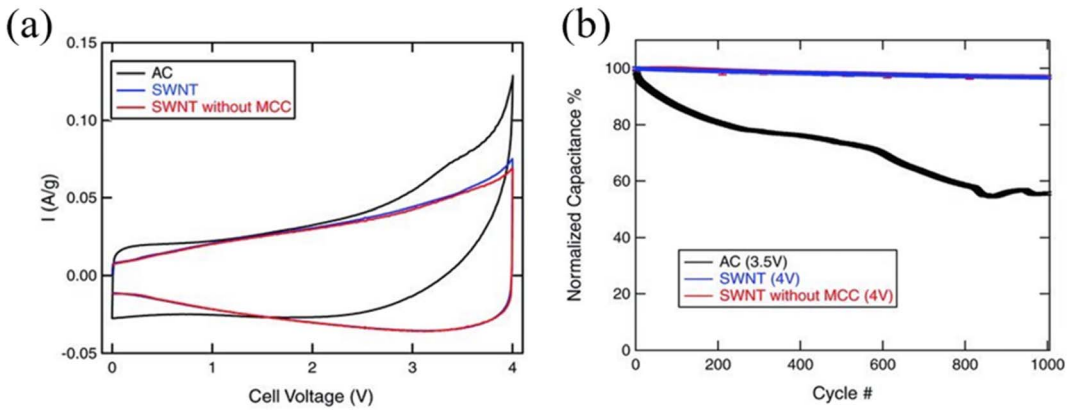

Fig. 6 (a) Cyclic voltammetry curves of AC, SWCNTs, and SWCNTs without MCC measured at 1 mV s^{-1} and (b) cycle stability over 1000 cycles at 1 A g^{-1}.[51] [This figure has been adapted/reproduced from ref. 51 with permission from John Wiley and Sons, copyright 2010.]

Another notable study on CNT-based high-voltage SCs includes opening of the CNT cap and shell of double or triple-walled CNTs by CO_2 etching which facilitated the organic electrolyte's ion transport through the inner wall of the CNTs, resulting in excellent SC performance under high-voltage conditions. Zheng *et al.* demonstrated the granulation of the double and triple-walled CNTs by CO_2 etching. After the etching process, the cap or side wall of the CNTs is opened and the specific surface area was increased (795 $m^2\ g^{-1}$) compared to that of the pristine CNTs (619 $m^2\ g^{-1}$). According to the pore distribution data, 3–10 nm pores are decreased after etching, 10–30 nm pores are increased and 1–2 nm pores are increased because of the cap and shell opening effects. The N_2 adsorption/desorption isotherm data show that the specific surface area was increased, which led to an increase in the charge storage capacity. As a result, CO_2 etched CNT-based SCs exhibited stable device performance at an operating voltage window of 4 V with a high specific capacitance of 57.9 F g^{-1} and stable cycling stability up to 5000 cycles. The initial loss of capacitance arose due to the presence of a metallic catalyst interacting with electrolyte while stable capacitance retention was observed after 1000 cycles (Fig. 7).[52] Previous research demonstrates that, to utilize the CNTs in high-voltage SCs, one needs to pay particular attention to remove the metallic impurities without introducing additional functional groups, controlling the CNT growth process to avoid the formation of amorphous carbon and to increase the SWCNTs to few-walled CNT content compared to the MWCNTs. Finally, exploring a method in which inner pores or the inner wall's surface area could be utilized for ion access would require further research efforts to achieve high-performance, stable, high-voltage SCs based on CNTs.

4.3 Graphene

Graphene is another widely researched active material for SCs. Graphene is a 2-dimensional (2D) material that consists of a single layer of sp^2 bonded carbon atoms arranged in a hexagonal lattice, which possesses exceptionally high electrical and thermal conductivity with high mechanical strength and physicochemical stability.[53] Considering the requirements of an active material for high-performance and stable SCs, graphene satisfies most of the requirements including high electrical conductivity, high specific surface area, high mechanical strength, and high thermal and chemical stability. Due to the many promising features of graphene, it has emerged as a high-capacity, high-performance EDLC electrode material over the past decade.[54] Until now, various forms of graphene-based materials have been utilized as active materials for high-voltage SC electrodes, including chemically modified graphene (CMG),[55] vertical graphene nanowalls,[56] reduced graphene oxide,[57] and graphene mesosponge sheets (GMSs).[58] Despite the great promise of graphene-based materials as active materials for EDLCs, under high-voltage conditions, graphene-based materials can meet certain challenges such as presence of metal impurities, amorphous carbon content, and presence of functional groups which could react with electrolyte to generate the unwanted side reaction which impact the long-term stability and the performance of the SCs. Amongst the various graphene candidates for high-voltage SCs, GMSs show exceptional performance in terms of operating voltage, which demonstrated stable SC operation up to 4.4 V at room temperature, one of the highest reported values for carbon-based active materials for SCs.[58] This work demonstrated the synthesis of functional group and metal impurity-free, highly-porous GMSs *via* two-stage high-temperature thermal processes under vacuum conditions involving alumina nanoparticle sheets as a catalyst. Moreover, the desired graphene structure was achieved by first, depositing a seed graphene layer on alumina *via* the conventional CVD process. The alumina support was then removed by the wet etching process using HF acid, generating mesoporous GMS powder, which was suitable for effective ion transport. The material was then further annealed at 1800 °C to form a continuous GMS structure (Fig. 8). By employing CVD processes using purified hydrocarbon sources, GMSs contained fewer functional groups with a smaller degree of amorphous content compared to the graphene synthesized from the widely used chemical exfoliation approach. Moreover, GMSs exhibited a highly mesoporous structure with a high specific surface area which is again highly desirable for high-voltage SCs. As a result, GMSs revealed a high specific surface area of 1500 $m^2\ g^{-1}$, a high total pore volume of 3.2 $cm^3\ g^{-1}$ and an excellent electrical conductivity of 18 S cm^{-1}. According to the Raman spectra of the GMS, it retained the characteristics of graphene (*e.g.*, D band, G band, and 2D band).

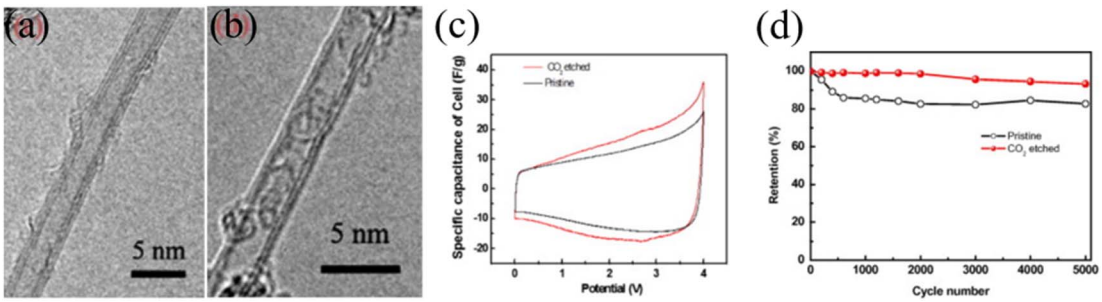

Fig. 7 TEM images of (a) TWCNTs and (b) DWCNTs, (c) CV curves of DWCNT/TWCNT electrodes in the range of 0 V–4 V, and (d) cycle retention of the etched CNT membrane and the pristine CNT membrane over 5000 cycles at 100 mV s^{-1}.[52] [This figure has been adapted/reproduced from ref. 52 with permission from Elsevier, copyright 2012.]

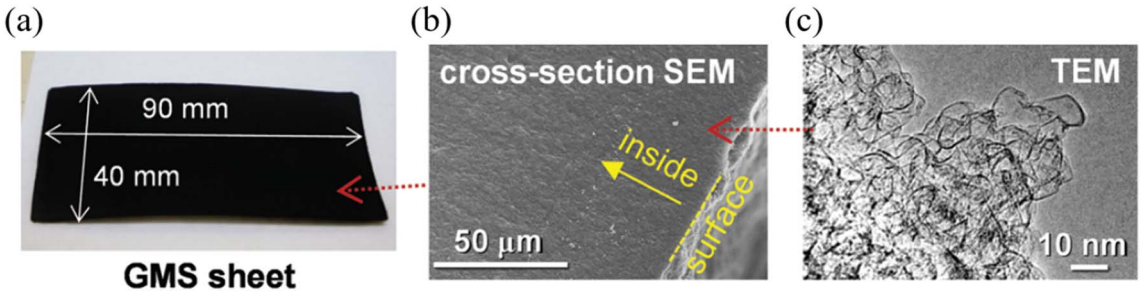

Fig. 8 (a) Photograph, (b) SEM and (c) TEM images of GMSs.[58] [This figure has been adapted/reproduced from ref. 58 with permission from the Royal Society of Chemistry, copyright 2019.]

Furthermore, CV curves of GMS-based SCs show that no electrolyte oxidation is observed from 0 V up to 3.5 V unlike the SWCNTs, rGO, and AC SCs, when 1.5 M triethylmethylammonium tetrafluoroborate (TEMA-BF_4)/propylene carbonate (PC) is used as the electrolyte. As a result, GMS-based SCs revealed stable SC performance at 4.4 V and excellent capacitance retention over 1000 cycles at 0–4.4 V, 1 A g^{-1} and stable capacitance retention over 100 000 cycles at 46 A g^{-1} (Fig. 9). Another notable study includes Chi *et al.* who demonstrated the synthesis and utilization of a vertically aligned (3D) graphene nanowall (GNW) directly grown on a Ti substrate as an electrode for high-voltage SCs. This work reveals the utilization of the pristine GNW as a positive electrode and the nitrogen-doped GNW as a negative electrode. Due to the synthesis of the vertically aligned graphene sheet in a controlled vacuum environment *via* the PECVD technique, vertically aligned graphene sheets contained a low degree of detrimental oxygen functional groups along with a decent graphitic quality of graphene (high sp^2 content). Furthermore, the lack of oxygen functional groups inhibited the generation of by-products such as CO and CO_2 gases and the presence of the N-doped GNW inhibited the hydrogen evolution reaction at the negative electrode (organic solvent degradation). As a result, asymmetric GNW-based SCs demonstrated stable performance up to 4 V with excellent cycling stability of nearly 100% retention over 10 000 cycles using a widely used organic electrolyte 1 M TEABF_4/PC, achieving a high energy density of 52Wh kg^{-1}.[56]

5. Future perspectives

5.1 Long-term stability

To realize high-performance, cost-effective SC-based ESSs, the long-term stability and energy density of the SCs are among the most important parameters. Long-term stability of SCs strongly

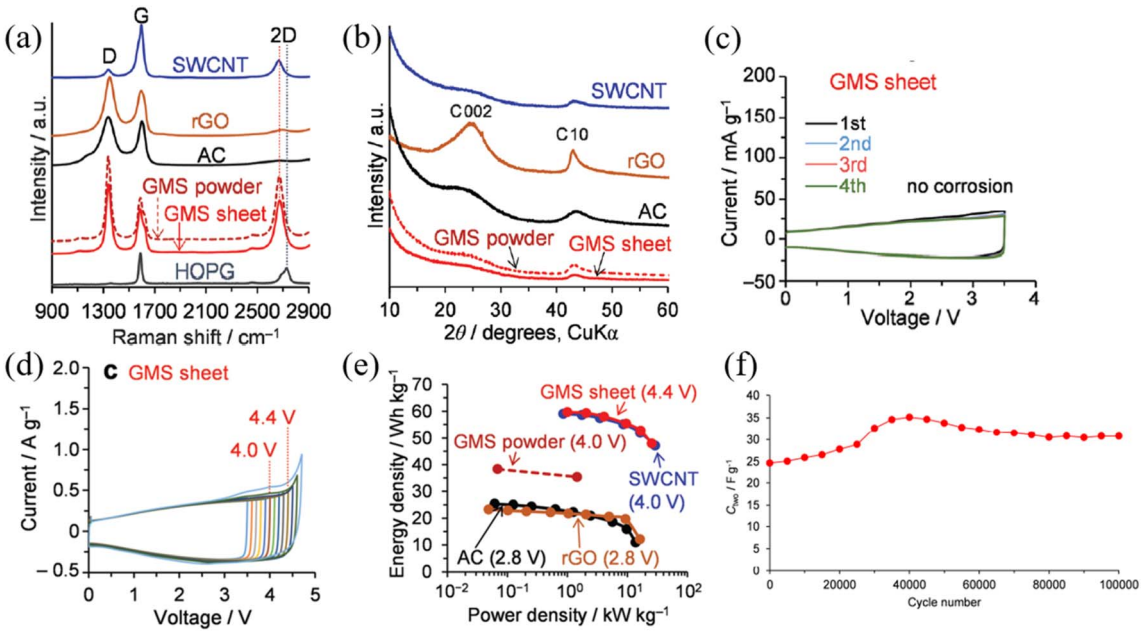

Fig. 9 (a) The Raman spectra, (b) XRD data of various carbon-based active materials, (c) CV curve of the GMS (0–3.5 V) at a scan rate of 1 mV s^{-1}, (d) CV curve of the GMS (0–4.4 V) at a scan rate of 10 mV s^{-1}, (e) Ragone plots of each carbon-based active material with the limit voltage, and (f) GMS cycle stability for 100 000 cycles at 46 A g^{-1} from 0 V to 4.4 V.[58] [This figure has been adapted/reproduced from ref. 58 with permission from the Royal Society of Chemistry, copyright 2019.]

Table 2 Features of the EDLC-based high-voltage SCs using carbon-based active materials[41,44,45,49,51,52,56,58]

Characteristics	Activated carbon	Carbon nanotubes	Graphene-based
Working voltage	3.2–4	4	4–4.4
Electrolytes	$TEABF_4$/acetonitrile	Et_4NBF_4/propylene carbonate	Et_3MeNBF_4/propylene carbonate
Specific energy density (Wh kg^{-1})	40–112	16–90	47.5–60
Specific power density (kW kg^{-1})	0.664–3.214	0.02–210	1–11.5
Cyclability (cycles)	5000–15 000	1000(SWCNTs) 5000 (MWCNTs)	1000 (100 000 for a fast scan rate)
Capacitance retention (%)	95–109	96.4 (SWCNTs) 95 (MWCNTs)	96–100
Specific surface area (m^2 g^{-1})	1000–3500	500–1300	450–1800

influences the life expectancy and the replacement cost of the ESSs while energy density determines the number of SC cells needed to be connected to deliver the required amount of the electrical energy output. The energy density and operating voltage influence the capital cost of ESSs and the long-term stability influences the operation cost of ESSs. As such, designing a SC at the cell level with long-term stability and wide operational voltage window becomes critical. So far, the previous studies suggest that there are areas of further research in each component level of SCs including the electrolyte and the carbon-based active material.

5.2 Electrolyte development

From the electrolyte perspective, various advanced organic electrolytes have been developed to widen the operating potential of the SCs, including the use of new organic solvents with a wider ESW and the use of new solvent and ion additives in the electrolytes. Furthermore, use of the inorganic additives and addition of a passivation layer on the electrode material have been found effective in widening the operating potential and improving the stability of the electrolyte. Key areas of future electrolyte research would be (1) discovering a new low-cost, organic electrolyte with a high ESW, (2) discovering a new, low-cost electrolyte additive which can enlarge the electrolyte ESW and finally (3) developing a new non-toxic, non-flammable electrolyte with a high ESW. Furthermore, combinatorial research effort in implementing both advanced electrolytes and an advanced electrode material and respective optimization effort would be needed in future to realize long-term stable, high-voltage SCs.

5.3 Electrode materials by design

Various advanced carbon-based materials have been utilized as an active material for high-voltage SCs. However, development of carbon-based nanomaterials which satisfy all the desirable criteria such as (1) functional group free, (2) metal impurity free, (3) low amorphous carbon, (4) scalable production, (5) low-cost, (6) highly mesoporous, (7) high specific surface area, (8) high electrical conductivity, and (9) good physicochemical and thermal stability remains a significant challenge and is an important area of future research. For example, as shown in Table 2, despite numerous research efforts in optimizing the AC, it still exhibits low electrical conductivity, high functional group contents with a lower operating voltage window along with low energy densities and poor cycling stabilities. In the case of more advanced carbon-based electrodes including the SWCNTs and graphene-based materials, they exhibit superior performances (Table 2) compared to AC in terms of higher electrical conductivity, operating voltage window, and energy densities along with improved long-term cycle stability in general. However, the modification or the synthesis of such advanced CNTs or graphene-based electrodes is not as scalable as the production of AC and it is more expensive compared to AC which hinders its widespread use at the industrial scale. Therefore, when developing an advanced carbon-based electrode material, one should carefully consider the complexity and the cost of material synthesis operation or modification processes while retaining all the excellent features which are desirable for EDLC-based high-voltage SCs.

6. Conclusion

To realize a carbon neutral society, increasing the use of renewable energy is inevitable, where a surge in demand for high-performance ESSs is predicted for the upcoming years. EDLC-based SCs will become an important segment in delivering highly effective short-term ESSs for rapid electrical power recovery and electrical power quality improvement. This mini-review discusses advances in EDLC-based SCs which could be suitable for the ESS application, placing strong importance on the long-term device stability and widening the operating voltage window which enhances the energy densities. Moreover, this mini-review provides insights into SCs at the component level such as electrolyte and active material-based perspectives on how one can enlarge the ESW of the electrolyte and how one can synthesize the active material with minimum functional groups and long-term device stability. Finally, this mini-review provides a future research area and the perspectives to enable the realization of high-performance, cost-effective SC-based ESSs for a future carbon-neutral society.

Author contributions

D. H. S., Z. H., K. K. L, and S. G. D. conceived and planned the work. J. M. L., Y. S. J., and J. S. K. contributed to writing of the materials and long-term device performance section. H. V. T. and K. K. L. contributed to the writing of the electrolyte section.

Y. H. Y., B. J. P, K. O., Z. H., and S. G. D contributed to the discussion and editing of the manuscript.

Conflicts of interest

The authors declare that they have no known competing financial interests for the work reported in this paper.

Acknowledgements

This work was primarily funded by the research support of Korea Institute of Energy Technology (KENTECH). D. H. S and S. G. D acknowledge the research support by the Korea Institute of Energy Technology Evaluation and Planning (KETEP) and the Ministry of Trade, Industry & Energy (MOTIE) of the Republic of Korea (No. 20224000000100). Z. H. acknowledges Future Fellowship (FT220100209) from the Australian Research Council. K. O. thanks the Australian Research Council and QUT Centre for Materials Science for partial support.

References

1 C. Figueres, C. Le Quere, A. Mahindra, O. Bate, G. Whiteman, G. Peters and D. Guan, *Nature*, 2018, **564**, 27–30.
2 Y. Yao, J. Lei, Y. Shi, F. Ai and Y.-C. Lu, *Nat. Energy*, 2021, **6**, 582–588.
3 M. Killer, M. Farrokhseresht and N. G. Paterakis, *Appl. Energy*, 2020, **260**, 114166.
4 I. Staffell, D. Scamman, A. Velazquez Abad, P. Balcombe, P. E. Dodds, P. Ekins, N. Shah and K. R. Ward, *Energy Environ. Sci.*, 2019, **12**, 463–491.
5 Q. Abbas, M. Mirzaeian, M. R. C. Hunt, P. Hall and R. Raza, *Energies*, 2020, **13**, 5847.
6 C. Schütter, S. Pohlmann and A. Balducci, *Adv. Energy Mater.*, 2019, **9**, 1900334.
7 A. González, E. Goikolea, J. A. Barrena and R. Mysyk, *Renewable Sustainable Energy Rev.*, 2016, **58**, 1189–1206.
8 S. Najib and E. Erdem, *Nanoscale Adv.*, 2019, **1**, 2817–2827.
9 Poonam, K. Sharma, A. Arora and S. K. Tripathi, *J. Energy Storage*, 2019, **21**, 801–825.
10 X. Chen, R. Paul and L. Dai, *Natl. Sci. Rev.*, 2017, **4**, 453–489.
11 W. Raza, F. Ali, N. Raza, Y. Luo, K.-H. Kim, J. Yang, S. Kumar, A. Mehmood and E. E. Kwon, *Nano Energy*, 2018, **52**, 441–473.
12 C. Zhong, Y. Deng, W. Hu, D. Sun, X. Han, J. Qiao and J. Zhang, *Electrolytes for Electrochemical Supercapacitors*, CRC Press, Boca Raton, 1st edn, 2016.
13 X. Wu, H. Yang, M. Yu, J. Liu and S. Li, *Mater. Today Energy*, 2021, **21**, 100739.
14 H. V. T. Nguyen, J. Kim and K. K. Lee, *J. Mater. Chem. A*, 2021, **9**, 20725–20736.
15 X. Wu, H. Yang, M. Yu, J. Liu and S. Li, *Mater. Today Energy*, 2021, 21.
16 B. Pal, S. Y. Yang, S. Ramesh, V. Thangadurai and R. Jose, *Nanoscale Adv.*, 2019, **1**, 3807–3835.
17 P. Ruschhaupt, S. Pohlmann, A. Varzi and S. Passerini, *Batteries Supercaps*, 2020, **3**, 698–707.
18 K. Xu, M. S. Ding and T. R. Jow, *J. Electrochem. Soc.*, 2001, **148**, A267–A274.
19 P. Azais, L. Duclaux, P. Florian, D. Massiot, M. A. Lillo-Rodenas, A. Linares-Solano, J. P. Peres, C. Jehoulet and F. Beguin, *J. Power Sources*, 2007, **171**, 1046–1053.
20 Y. H. Liu, B. Rety, C. M. Ghimbeu, B. Soucaze-Guillous, P. L. Taberna and P. Simon, *J. Power Sources*, 2019, **434**, 226734.
21 P. Kurzweil, J. Schottenbauer and C. Schell, *J. Energy Storage*, 2021, 35.
22 M. Zhu, C. J. Weber, Y. Yang, M. Konuma, U. Starke, K. Kern and A. M. Bittner, *Carbon*, 2008, **46**, 1829–1840.
23 F. H. Zheng, Y. X. Li and X. S. Wang, *Electrochim. Acta*, 2018, **276**, 343–351.
24 P. Kurzweil and M. Chwistek, *J. Power Sources*, 2008, **176**, 555–567.
25 S. Ishimoto, Y. Asakawa, M. Shinya and K. Naoi, *J. Electrochem. Soc.*, 2009, **156**, A563–A571.
26 A. Brandt, P. Isken, A. Lex-Balducci and A. Balducci, *J. Power Sources*, 2012, **204**, 213–219.
27 K. Chiba, T. Ueda, Y. Yamaguchi, Y. Oki, F. Saiki and K. Naoi, *J. Electrochem. Soc.*, 2011, **158**, A1320–A1327.
28 K. Chiba, T. Ueda, Y. Yamaguchi, Y. Oki, F. Shimodate and K. Naoi, *J. Electrochem. Soc.*, 2011, **158**, A872–A882.
29 H. V. Nguyen, A. Bin Faheem, K. Kwak and K. K. Lee, *J. Power Sources*, 2020, **463**, 10.
30 S. Pohlmann, T. Olyschlager, P. Goodrich, J. A. Vicente, J. Jacquemin and A. Balducci, *J. Power Sources*, 2015, **273**, 931–936.
31 V. L. Martins, A. J. R. Rennie, N. Sanchez-Ramirez, R. M. Torresi and P. J. Hall, *Chemelectrochem*, 2018, **5**, 598–604.
32 M. Pohl, I. Tallo, A. Janes, T. Romann and E. Lust, *J. Power Sources*, 2018, **402**, 53–61.
33 H. V. Nguyen, S. Lee, K. Kwak and K. K. Lee, *Electrochim. Acta*, 2019, **321**, 9.
34 F. C. Krause, J. P. Jones, M. C. Smart, K. B. Chin and E. J. Brandon, *Electrochim. Acta*, 2021, 374.
35 J. Yao, M. W. Shi, W. S. Li, Q. K. Han, M. S. Wu, W. Yang, E. G. Wang and X. M. Lu, *Chemelectrochem*, 2022, 9.
36 K. L. Van Aken, M. Beidaghi and Y. Gogotsi, *Angew. Chem., Int. Ed.*, 2015, **54**, 4806–4809.
37 F. Yao, D. T. Pham and Y. H. Lee, *ChemSusChem*, 2015, **8**, 2284–2311.
38 L. Wei and G. Yushin, *Nano Energy*, 2012, **1**, 552–565.
39 L. Luo, Y. Lan, Q. Zhang, J. Deng, L. Luo, Q. Zeng, H. Gao and W. Zhao, *J. Energy Storage*, 2022, **55**, 105839.
40 K. Kierzek, E. Frackowiak, G. Lota, G. Gryglewicz and J. Machnikowski, *Electrochim. Acta*, 2004, **49**, 1169–1170.
41 M. S. Balathanigaimani, W.-G. Shim, M.-J. Lee, C. Kim, J.-W. Lee and H. Moon, *Electrochem. Commun.*, 2008, **10**, 868–871.
42 J. Pallarés, A. González-Cencerrado and I. Arauzo, *Biomass Bioenergy*, 2018, **115**, 64–73.
43 Q. Li, R. Jiang, Y. Dou, Z. Wu, T. Huang, D. Feng, J. Yang, A. Yu and D. Zhao, *Carbon*, 2011, **49**, 1248–1257.

44 M. Vijayakumar, A. Bharathi Sankar, D. Sri Rohita, K. Nanaji, T. Narasinga Rao and M. Karthik, *ChemistrySelect*, 2020, **5**, 8759–8772.
45 D. Gandla, X. Wu, F. Zhang, C. Wu and D. Q. Tan, *ACS Omega*, 2021, **6**, 7615–7625.
46 Y. P. Guo, J. R. Qi, Y. Q. Jiang, S. F. Yang, Z. C. Wang and H. D. Xu, *Mater. Chem. Phys.*, 2003, **80**, 704–709.
47 H.-J. Peng, J.-Q. Huang, M.-Q. Zhao, Q. Zhang, X.-B. Cheng, X.-Y. Liu, W.-Z. Qian and F. Wei, *Adv. Funct. Mater.*, 2014, **24**, 2772–2781.
48 G. Chen, D. N. Futaba, S. Sakurai, M. Yumura and K. Hata, *Carbon*, 2014, **67**, 318–325.
49 A. Peigney, C. Laurent, E. Flahaut, R. R. Bacsa and A. Rousset, *Carbon*, 2001, **39**, 507–514.
50 L. L. Zhang, R. Zhou and X. S. Zhao, *J. Mater. Chem.*, 2010, **20**, 5983–5992.
51 A. Izadi-Najafabadi, S. Yasuda, K. Kobashi, T. Yamada, D. N. Futaba, H. Hatori, M. Yumura, S. Iijima and K. Hata, *Adv. Mater.*, 2010, **22**, E235–E241.
52 C. Zheng, W. Qian, C. Cui, Q. Zhang, Y. Jin, M. Zhao, P. Tan and F. Wei, *Carbon*, 2012, **50**, 5167–5175.
53 Y. Huang, J. Liang and Y. Chen, *Small*, 2012, **8**, 1805–1834.
54 S. W. Bokhari, A. H. Siddique, P. C. Sherrell, X. Yue, K. M. Karumbaiah, S. Wei, A. V. Ellis and W. Gao, *Energy Rep.*, 2020, **6**, 2768–2784.
55 M. D. Stoller, S. Park, Y. Zhu, J. An and R. S. Ruoff, *Nano Lett.*, 2008, **8**, 3498–3502.
56 Y.-W. Chi, C.-C. Hu, H.-H. Shen and K.-P. Huang, *Nano Lett.*, 2016, **16**, 5719–5727.
57 S. Shivakumara, B. Kishore, T. R. Penki and N. Munichandraiah, *ECS Electrochem. Lett.*, 2015, **4**, A87.
58 K. Nomura, H. Nishihara, N. Kobayashi, T. Asada and T. Kyotani, *Energy Environ. Sci.*, 2019, **12**, 1542.